Paramagnetic spectral response of $CePd_3$: A comparative investigation of neutron inelastic scattering from single-crystal and polycrystalline samples

A. P. Murani, A. Severing, and W. G. Marshall
Institut Laue-Langevin, 156x, 38042 Grenoble Cedex, France
(Received 27 March 1995; revised manuscript received 5 July 1995)

We report a comparative neutron inelastic-scattering study of single-crystal and polycrystalline samples of $CePd_3$ with the aim to resolve conflicting claims concerning the form of the *paramagnetic* spectral response of the compound. The present measurements show that the inelastic scattering particularly at *low scattering angles* is very similar for both samples. We find also that the observed scattering at energies below 30 meV is mostly nonmagnetic. At low angles it is dominated by multiple-scattering processes in the relatively large samples used for the measurements. Magnetic scattering occurs predominantly at high energies and can be represented by a single-ion spectral function centered on a characteristic energy of ~50–55 meV, in good accord with previous findings from time-of-flight and polarized neutron measurements on a triple-axis spectrometer.

INTRODUCTION

Valence fluctuation phenomena have been investigated theoretically and experimentally with considerable interest during the last two decades. While progress in understanding the physical origin of the underlying phenomena has been made, considerable work both experimental and theoretical still remains to be done especially since the subject has often been clouded by controversies in a number of domains as for example photoemission, Bremstrahlung isochromat spectroscopy as well as neutron scattering, amongst others. It is, of course, important to address these controversies with a view to reaching consensus on reliable experimental facts to check against existing theories and so provide impetus for further work and understanding of the subject.

In the following we examine the question regarding the form of the low-temperature spectral response associated with Ce ions in the classic valence fluctuation compound $CePd_3$ concerning which conflicting claims have been made in the literature. Measurements on a single-crystal sample performed by Shapiro, Stassis, and Aeppli (referred to hereafter as SSA) using a triple-axis spectrometer[1] were interpreted as showing magnetic scattering mainly at low energies and analyzed in terms of two Lorentzian components centered on zero energy (i.e., a quasielastic distribution) with a spectral half-width of 3 ± 2 meV and another on ~16 meV with a half-width of ~12 meV. This finding, however, contrasts markedly with the broad high-energy single-ion spectral response (viz. a Lorentzian) centered on a characteristic Kondo energy of ~55 meV (half-width ~40 meV) observed from earlier measurements on a polycrystalline sample using the time-of-flight technique as well as with polarized neutrons on a triple-axis spectrometer.[2–4]

We have undertaken an extensive neutron inelastic-scattering investigation of this compound and report below the results obtained with the time-of-flight technique on the same single-crystal sample of $CePd_3$ as used earlier for the measurements reported in Ref. 1, as well as on a polycrystalline powder of $CePd_3$. The latter was packed, using a thin aluminum foil, into a cylinder of similar dimensions as the single crystal, viz. 5 mm diameter and ~40 mm length, in order to keep the geometrical shape-dependent effects such as multiple scattering closely similar for both samples. This is important since, as shown below, multiple-scattering processes dominate the observed nonmagnetic scattering at low angles. Although one could also observe coherent single phonon scattering at low angles if the Q-ω trajectory (see the Appendix) meets a phonon-dispersion branch, the cross section of such a mode (proportional to Q^2) is relatively low due to the low value of Q (~1.2 $Å^{-1}$ for $\omega<30$ meV and $E_i=115$ meV) for the scattering angle of 10°. In the case of the polycrystalline sample the relative intensity of the single-phonon scattering is even further reduced due to polycrystalline $|Q|$ averaging and is negligible in comparison with the multiple-scattering contributions in the relatively large samples used for the measurements.

LOW-TEMPERATURE RESULTS

In the time-of-flight neutron inelastic-scattering technique a regular sequence of sharp pulses of monochromatic neutrons impinges on a sample and the scattered neutrons are collected and time analyzed within a bank of detectors covering a wide angular range. The time-analyzed data are converted to cross section on the energy scale via a straightforward transformation. In Fig. 1 we show the observed scattering at 10 K at low angles $\langle 2\Theta\rangle=9.5°$ (covering the angular range between 6.5 and 12.5 degrees) from the single-crystal sample as well as ''background scattering'' measured under identical conditions with only the sample removed. The incident neutron energy of 115 meV used in the present measurements is comparable to the incident neutron energy *at the high energy end* ($\omega=80$ meV) of the triple-axis scan[1] close to the zone center at $\mathbf{q}=(0, 0.1, 0.1)$ with $\mathbf{Q}=(2, 1.1, 1.1)$, i.e., $Q=3.9$ $Å^{-1}$. The measurements were performed with a fixed final energy E_f of 30.5 meV. The results of the latter investigation are shown in Fig. 2. In that experiment

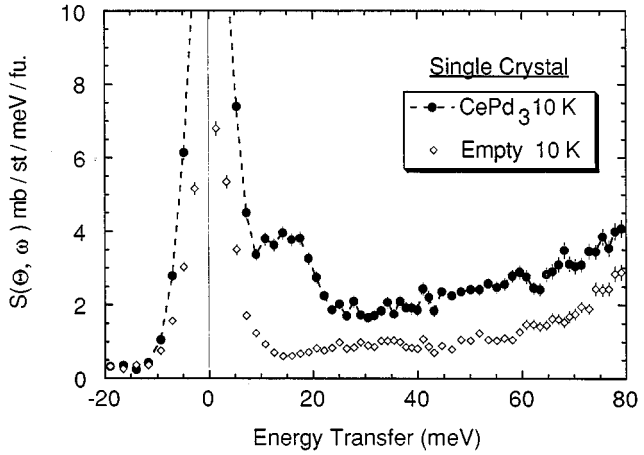

FIG. 1. Time-of-flight raw data converted to $S(\Theta, \omega)$ for the $CePd_3$ single crystal (black points) as well as the "empty cell" (diamonds). Both data sets represent low angle scattering at $\langle 2\Theta \rangle = 9.5°$ measured at 10 K using neutrons of incident energy 115 meV.

the low-energy region below 40 meV was measured at a lower $\mathbf{Q}=(0, 1.1, 1.1)$, i.e., $Q=2.4$ Å^{-1}, but the same value of $\mathbf{q}=(0, 0.1, 0.1)$. At this lower $\mathbf{Q}$ the Ce^{3+} form factor is ~35% larger and the intensity of the optic phonon ~2.6 times smaller. The present time-of-flight (tof) measurements were performed with the incident wave vector $\mathbf{k_i}$ along the [0,1,1] direction, but within the accuracy of our experiment the observed scattering at *low angles* was independent of the incident direction of $\mathbf{k_i}$ as seen from the fact that the observed scattering remained unmodified when the sample was

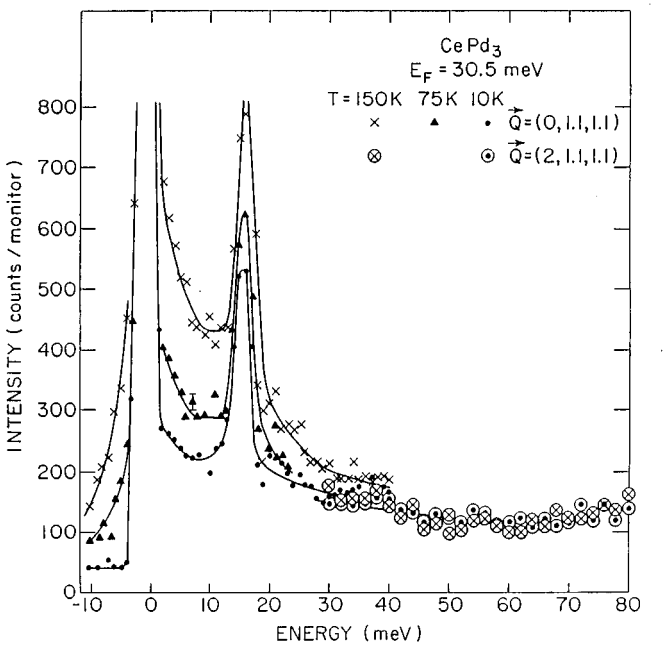

FIG. 2. The temperature dependence of the inelastic scattering measured by SSA (Ref. 1) on the same single crystal of $CePd_3$ as used in the present experiments. The measurements were performed at constant $\mathbf{Q}$'s with $\mathbf{q}=(0, 0.1, 0.1)$ in two different Brillouin zones.

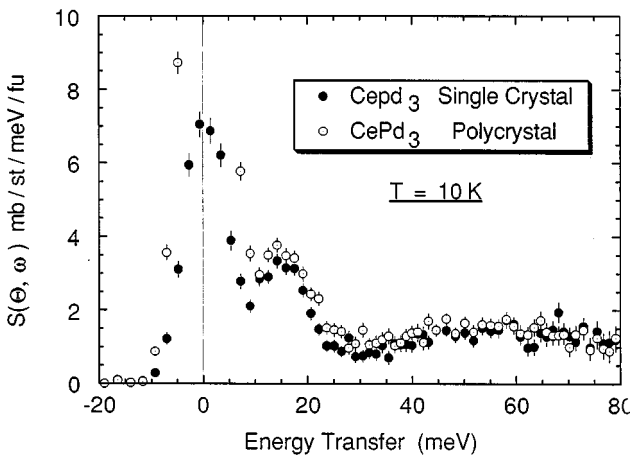

FIG. 3. Low angle data at 10 K for the single-crystal and polycrystalline samples of $CePd_3$ after correcting identically for the "empty cell" scattering. The (resolution broadened) incoherent elastic scattering is significantly larger for the polycrystal which also shows a slightly more pronounced inelastic scattering within the hump centered on ~10–15 meV. The scattering above ~30 meV is, however, closely similar for the two samples.

rotated through 15°. The scattered neutrons were counted within a bank of detectors covering the angular range between 6° and ~100°. In Figs. 10 and 11 of the Appendix we illustrate the scattering diagrams in the reciprocal space in the present tof as well as the three-axis measurements of SSA.[1]

In Fig. 3 we show the low angle (9.5°) time-of-flight data for both the single-crystal and powder samples of $CePd_3$ after a one to one background subtraction. Both data sets were normalized with respect to the scattering from a composite vanadium sample consisting of two plates of thickness 1 mm each. The open circles in Fig. 3 represent scattering from the polycrystal, while the black dots that from the single-crystal sample. Similar results for the high angle detector bank (at 88°) are shown in Fig. 4. The form of the inelastic scattering at high angles is very similar for both samples, albeit a little

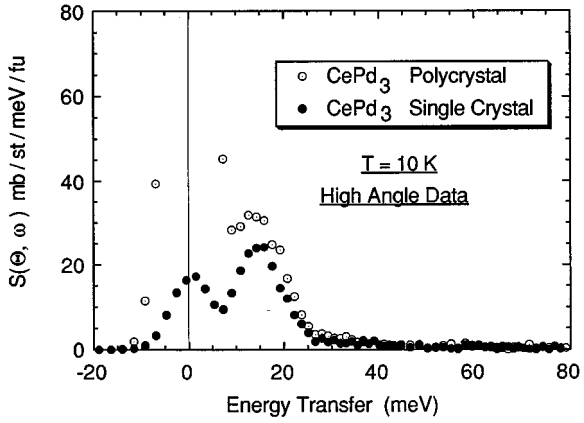

FIG. 4. High angle data at 10 K for the single-crystal and polycrystal samples of $CePd_3$. Note the difference in the vertical scale compared with Fig. 3, and the relatively weak high-energy scattering above ~40–50 meV.

weaker for the single crystal, while the elastic scattering is very much stronger for the polycrystal compared with the single crystal. This is because in the case of the polycrystalline powder sample the scattering triangles at $\omega=0$ for some of the detectors within this particular group of high angle detectors at 88° (average angle) meet some of the Debye-Scherrer rings, while for the single crystal none of the detectors within the same angular range satisfy the Bragg condition.

We see from Fig. 3 that the elastic scattering from the polycrystalline powder is stronger than for the single crystal for the low angle data also. Few Debye-Scherrer rings are ''cut'' at these low angles so that the increased elastic scattering is due partly to increased multiple scattering as well as increased surface scattering from a powder possibly enhanced by contamination of the surface by moisture from the air. However, the *inelastic* scattering at low angles is similar for both samples particularly at high energies, represented by the broad hump centered on ~50–60 meV. It should be noted that this high-energy scattering is negligibly small in the high angle data while the component centered around ~10–15 meV is similar but higher in intensity, roughly a factor 8 to 9 higher compared with the low angle data.

A clear understanding of the origin of this low-energy inelastic scattering (centered on 10–15 meV) is the key to an understanding of the paramagnetic spectral response from $CePd_3$. We suggest that the low-energy inelastic scattering is mainly of ''phononic'' origin and at low angles is due mainly to multiple-scattering processes (in which the dominant contribution is via double scattering processes where the first scattering event is along the axis of the cylindrical sample). This is because for single-phonon processes the scattering should scale as Q^2 so that for the two angles of 9.5° and 88° we should expect a difference in intensity of a factor of ~70. In other words the scattering intensity in the low angle data relative to the high angle should be much smaller (~1/70th) than actually observed (~1/9th) if it were due to single-phonon events. One must then consider whether a small fraction of the ''additional scattering'' above the 1/70th level of the high angle scattering (expected from the Q^2 scaling) might correspond to magnetic contributions similar to those ''identified'' in the experiments of Shapiro *et al.*

We have addressed this question and investigated the low-energy region in more detail using lower incident energy neutrons. Results for the single-crystal sample obtained with neutrons of incident energy 17 meV are shown in Fig. 5, where the black circles represent the as-measured signal and diamonds the ''background'' scattering, i.e., the observed scattering at the same temperature with only the sample removed from its holder (as done also for the higher incident energy measurements). The difference scattering shown by the open circles is rather weak and contrasts markedly with the strong hump centered around 10–15 meV seen in the higher energy measurements. The two sets of data at 115 and 17 meV have been taken sequentially (with the sample remaining undisturbed) and normalized with respect to the measured scattering from the same vanadium standard also measured sequentially at both incident neutron energies, making the vertical scale independent of instrumental parameters such as the energy resolution. Hence, the observed intensities, which are on absolute scale, can be directly compared between the 17 and 115 meV data.

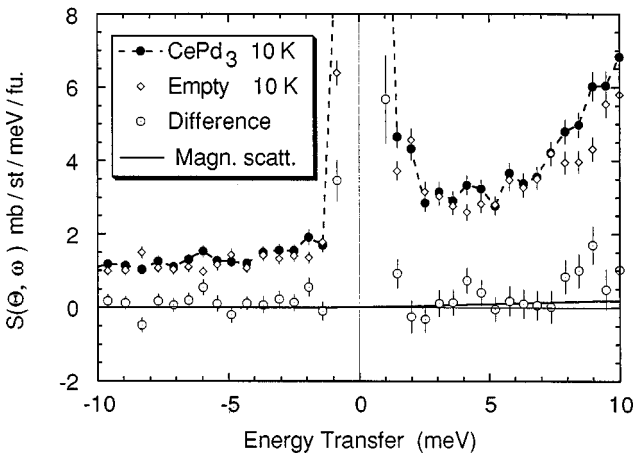

FIG. 5. Low energy data for the $CePd_3$ single crystal obtained with neutrons of incident energy 17 meV (black points) and the ''empty cell'' (diamonds) with the difference scattering shown by the open circles. The solid line shows the magnetic contribution calculated using the parameters of the KMH fit performed on the high energy data, Fig. 8.

Thus, even if the whole of the difference scattering (i.e., the real signal) measured with 17 meV neutrons is attributed to magnetic contribution it is clear that the latter is rather weak, in fact much weaker than the scattering reported by Shapiro *et al.* In the latter experiment the final neutron energy was kept fixed at 30.5 meV, hence the incident neutron energy varied from ~30 meV at zero energy transfer to ~45 meV at $\omega=15$ meV and ~110 meV at $\omega=80$ meV. From a comparison of the low-energy (17 meV) and high-energy (115 meV) data reported here it is clear that the observed difference in the scattering in the low-energy region (centered on 10–15 meV) between the two sets is related to the magnitude of the incident energy employed since any variation via the magnetic form factor for the $|Q|$ vectors involved would be relatively small.

The results obtained with 17 meV neutrons show not only that the magnetic scattering is weak but also any nonmagnetic contribution is similarly rather weak. The reason for the weakness of the latter, discussed in the Appendix (Fig. 13), is that few phonon branches are cut for scattering angles around 10° so that the single-phonon scattering contribution is negligible. Also, the overall multiple scattering is rather weak since, as seen from Fig. 13, relatively few phonon branches are cut along 90° also, and since the dominant contribution to multiple scattering arises via processes in which the first scattering events are along the axis of the cylindrical samples.

In Fig. 6(a) we show a fit (including convolution with the Gaussian instrumental energy resolution function) to the single-crystal data assuming a δ function centered on zero energy for the inelastic scattering and two *inelastic* spectral components with a Gaussian distribution for the low energy inelastic hump and a Lorentzian to represent the broad higher energy scattering. In Fig. 6(b) we show a similar fit to the high angle data (average angle 88°) assuming only one inelastic component (the lower energy Gaussian) plus the zero-energy δ function. As noted above, at this angle the broad

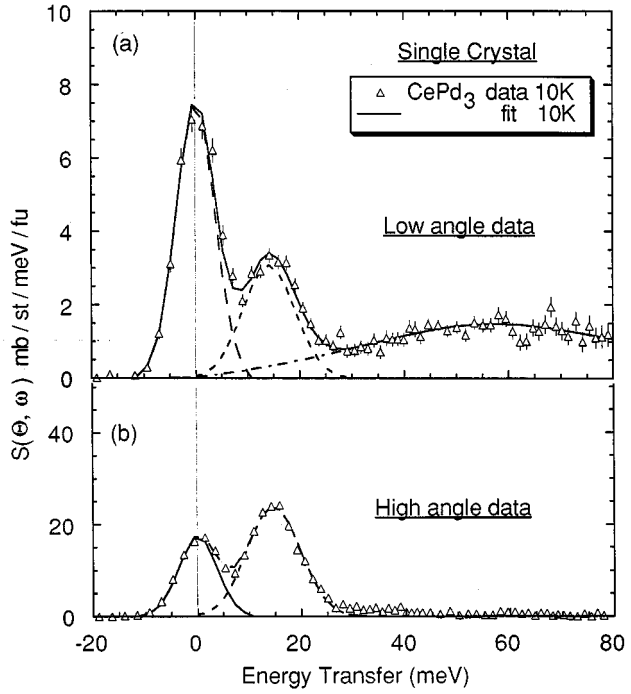

FIG. 6. Scattering at 10 K from the $CePd_3$ single-crystal sample for (a) $\langle 2\Theta\rangle = 9.5°$ and (b) $\langle 2\Theta\rangle = 88°$ detector banks. The data have been fitted after convolution with a Gaussian energy resolution function, assuming a δ function for the elastic scattering, a Gaussian spectral distribution for the low energy hump, and a Lorentzian for the broad high energy hump which has negligibly small intensity at high angles.

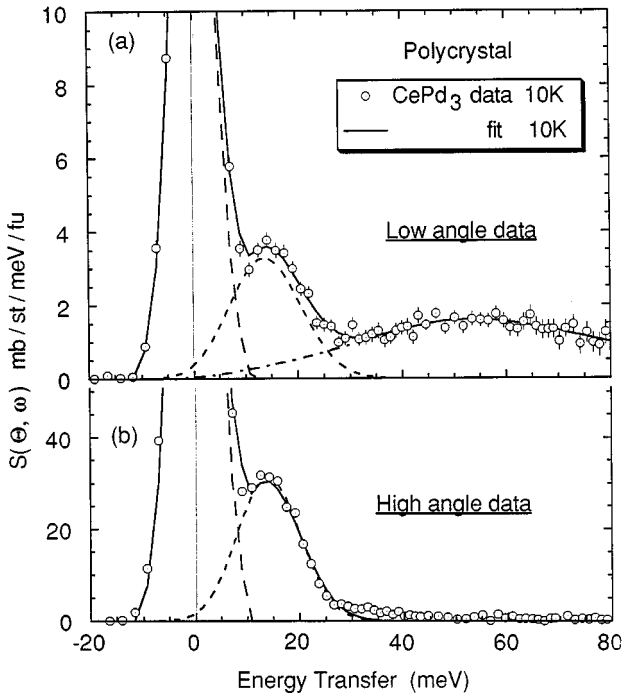

FIG. 7. $CePd_3$ polycrystalline data and fits similar to those in Fig. 6.

high-energy distribution has practically disappeared while the low energy inelastic hump (centered on ~10–15 meV) has increased in intensity significantly. A detailed examination of the data shows that the high-energy scattering decreases progressively with increasing scattering angle (increasing Q) as expected from the magnetic form factor dependence. In view of this we have included, with the fitted Lorentzian spectral component, the Ce^{3+} form-factor variation of intensity as a function of energy transfer ω and hence Q for a fixed scattering angle. The variation of Q with ω (i.e., the Q-ω trajectory) is shown in Fig. 12 of the Appendix.

Results of similar fits to the low and high angle data for the powder sample are shown in Fig. 7. As mentioned previously, the elastic scattering at high angles for the polycrystal is greatly enhanced relative to the low angle while the increase is smaller for the single crystal (Fig. 5). The phonon scattering, in the high angle data represented by the broad inelastic hump, is a little stronger in intensity, broader in width and centered on a lower energy for the powder sample. The high-energy scattering centered on ~50–60 meV is almost identical for both samples indicating that the difference between the two is principally at energies below 30 meV, particularly in the region of the elastic scattering. In the Appendix, Fig. 12 we show the Q-ω trajectories followed in the two experiments as well as the phonon-dispersion curves[5] along the $[0,\zeta,\zeta]$ direction. Also, as seen from Fig. 11, in the tof experiment $\mathbf{Q}$ varies with energy transfer ω and is not confined to any specific direction. However, the situation in relation to phonons is qualitatively similar for the other two principal directions.

In sum, from our measurements with 115 meV neutrons we have found the ratios of the observed intensity of the broad ''phonon humps'' between the low (9.5°) and the high angle (88°) detector banks to be $8(\pm 0.5)$ and $9(\pm 0.5)$ for the single-crystal and polycrystalline samples, respectively, while the normal Q^2 scaling for single-phonon processes would suggest the ratio should be ~70. Thus single-phonon processes contribute only about 10% of the observed nonmagnetic intensity in the low angle bank. The rest of the signal we attribute to multiple-scattering processes in the *large* cylindrical samples of diameter 5 mm and length 40 mm. A strong channel for these involves scattering through 90° along the axis of the cylinder which provides the longest path within the sample for neutrons scattered once and hence also the greatest probability for a second scattering event through a similarly large angle into the low angle detector bank. It is interesting to note also that the form (shape) of the inelastic nonmagnetic scattering is similar at both low and high angles so that a constant fraction of the high angle scattering can represent fairly closely the nonmagnetic contribution in the low-angle bank. We have therefore used the constant fractions mentioned above to subtract out the nonmagnetic contributions for both samples in the data presented below.

ANALYSIS OF THE MAGNETIC SIGNAL

The ''phonon'' (i.e., nonmagnetic scattering) corrected data represented by open circles and black dots thus obtained are shown in Fig. 8 where the continuous curve represents a

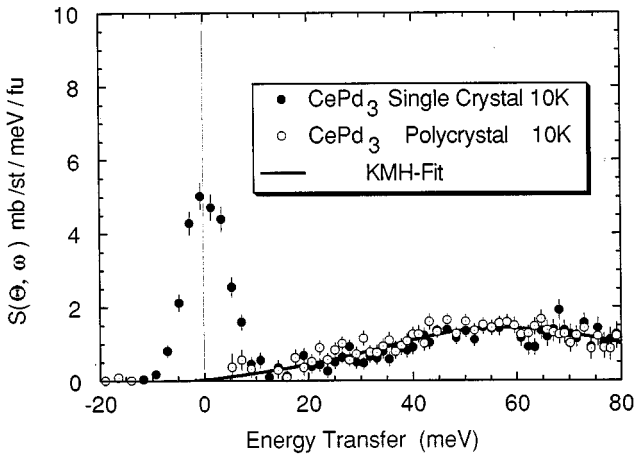

FIG. 8. Low angle magnetic scattering evaluated assuming the nonmagnetic contributions to be given by a constant fraction of the high angle scattering. The solid line represents the best fit to the two data sets taken together, using the KMH spectral function.

least-squares fit to the data using the *single-ion* spectral function for the Anderson impurity given by Kuramoto and Müller-Hartmann (KMH),[6] viz.

$$S(Q,\omega)=\frac{C\chi(Q)F^2(Q)}{[1-\exp(-\omega/T)]}\frac{\alpha\omega}{u^2(u^2+4\alpha^2)}\times\left\{\alpha\ \ln[(1-u^2)^2+4u^2\alpha^2]+|u|\left[\frac{\pi}{2}-\tan^{-1}\left(\frac{1-u^2}{2|u|\alpha}\right)\right]\right\}, \quad (1a)$$

where C is a constant, $\chi(Q)$ is the static susceptibility, $F(Q)$ is the magnetic form factor, and $[1-\exp(-\omega/T)]^{-1}$ is the detailed balance factor. The frequency ω and temperature T are in the (same) energy units with $u=\omega/\omega_0$, where ω_0 represents the characteristic energy and $\alpha=\sin(\pi\langle n_f\rangle/N)$, with $\langle n_f\rangle$ the occupancy and N the degeneracy of the $4f$ state. The fit yields $\omega_0=50$ (±5) meV and $\alpha=0.51\pm0.03$ from which we obtain $\langle n_f\rangle=0.9\pm0.05$, assuming the degeneracy $N=6$. The characteristic energy $\omega_0\sim50$ meV is fairly similar or slightly smaller than the observed centroid of the Lorentzian at ~55 meV reported earlier by Galera and co-workers[2,3] as well as from the Lorentzian fit to the present single-crystal data, represented by

$$S(Q,\omega)=\frac{C'\chi(Q)F^2(Q)}{[1-\exp(-\omega/T)]}\frac{\omega}{[\Gamma^2+(\omega-\omega_0)^2]}, \quad (1b)$$

where Γ is the Lorentzian half-width at half maximum.

Neutron-scattering measurements on a number of valence fluctuation systems spanning a wide range of characteristic energies as for example, $YbAgCu_4$ ($T_K\sim10$ meV),[7] $CeSn_3$ ($T_K\sim40$ meV),[8] $YbInCu_4$ ($T_K\sim40$ meV),[9] α-Ce ($T_K\sim170$ meV),[10,11] normally show a similar Lorentzian-like single-ion spectral response centered on the characteristic energy ω_0. Theories for the Kondo lattice suggest that in the large-N limit the Kondo-lattice ground state is well approximated by a lattice of uncorrelated Kondo singlets.[12,13] The characteristic energies T_K or T_f (commonly referred to as Kondo energies or spin-fluctuation energies) obtained from the neutron data are in good quantitative accord with the Fermi-liquid relations linking γ and $\chi(0)$ with T_K, viz. $\gamma=\pi^2k_B^2\langle n_f\rangle/3\omega_0$ and $\chi(0)=\mu^2\langle n_f\rangle/3\omega_0$, where $\omega_0=T_K$ or T_f and $\mu^2=g_J^2J(J+1)\mu_B^2$. They provide an essential cross check for the single-ion character of the magnetic response. In the case of $CePd_3$ assuming $\langle n_f\rangle=0.83$ (±0.05) obtained from the $L_{\rm III}$ absorption measurements[14,15] and $T_K=50$ (±5) meV from the KMH fit we obtain $\gamma\sim39$ (±4) mJ mol^{-1} K^{-2} in excellent agreement with the literature value[16] of $\gamma=39$ mJ mol^{-1} K^{-2}. Also, we obtain $\chi(0)=1.2$ (±0.15)$\times10^{-3}$ emu mol^{-1} in reasonable accord with $\chi(0)=1.4\times10^{-3}$ emu mol^{-1} obtained by Kappler *et al.*[17] which is close to that found for our polycrystalline sample.[3] In both cases corrections have been applied to the bulk susceptibility data for the low-temperature Curie-Weiss upturn (tail) often attributed to extrinsic or impurity effects or to Ce moments stabilized (i.e., having lower T_K's) by defects or imperfections within the surrounding near-neighbor shell. Fermi-liquid scaling of the magnetic response of $CePd_3$ was demonstrated by Galera *et al.*[3] but the result, and particularly the observed magnitude of T_K (~600 K) is frequently ignored in favor of a "Kondo or spin fluctuation" temperature T_f of ~250 K.[18–20]

In another investigation on a polycrystalline $CePd_3$ sample[21] the absolute calibration of the cross section performed with reference to a standard vanadium gave excellent agreement with the static bulk susceptibility and an integrated spectral intensity of ~280 mb sr^{-1} Ce^{-1} consistent with a $4f$ occupancy $\langle n_f\rangle$ of ~0.85, obtained from the $L_{\rm III}$ absorption measurements.

The above-mentioned repeated observations of broad single-ion spectral response in $CePd_3$ centered on the characteristic energy of ~50–55 meV are at variance with constant-q energy scans close to the Brillouin zone center at $\mathbf{Q}=(0, 1.1, 1.1)$ on the single-crystal sample performed by SSA.[1] The latter showed an optic phonon at ~15 meV riding on top of the broad low-energy scattering which was *assumed to be magnetic* and analyzed in terms of a quasielastic Lorentzian spectrum of width ~3 meV plus an inelastic Lorentzian centered on ~16 meV and width ~12 meV. Converting these data to absolute scale, by calibration relative to an acoustic phonon, SSA (Ref. 1) found that the Kramers-Kronig integrals of these two spectral components together yield $\chi(0)\sim1.7\times10^{-3}$ emu mol^{-1} in reasonable accord with the bulk susceptibility of $CePd_3$. However, working from this susceptibility calibration together with the energy parameters of the two Lorentzian spectral components of their fits, we have evaluated the integrated cross section of the "magnetic" scattering and find it to be *very low*, only ~33 mb sr^{-1} Ce^{-1} if the integration is limited to the measured energy range, i.e., 80 meV, or 44 mb sr^{-1} Ce^{-1} obtained by integrating the fitted functions to 200 meV. The cross section can be as high as ~54 mb sr^{-1} Ce^{-1} if the integration is extended up to 500 meV. Even the last value is only 1/6th of the cross section of 314 mb sr^{-1} for the Ce^{3+} ion and corresponds to a rather low $4f$ occupancy $\langle n_f\rangle\sim0.17$.

The reason why both the present data and those of Ref. 1 yield similar values for the susceptibility but give markedly different moments is, of course, rather simple. As discussed below [Eq. (3)] the spectral function $S(\omega)$ is related to $\chi''(\omega)$ via the relation, $S(\omega)=(2\pi)^{-1}\ [1-\exp(-\omega/T)]^{-1}\chi''(\omega)$. As

$T \to 0$ K the detail balance factor $[1-\exp(-\omega/T)]^{-1}$ approaches unity for $+ve\ \omega$, so we have $\chi''(\omega) \cong S(\omega)$, where for simplicity we have put $(2\pi)^{-1}=1$. Now, while the moment integral is simply $\int S(\omega)d\omega$ the Kramers-Kronig integral (at low T) becomes $\int [S(\omega)/\omega]d\omega$. Hence low-energy spectral components contribute much more weight (proportional to $1/\omega$) to the susceptibility compared with the moment integral.

An important observation from our tof measurements on the large single-crystal of $CePd_3$ is that a significant amount of multiple scattering occurs at low Q's (i.e., low angles). This is represented by the broad ''phononic hump.'' From the present results we have evaluated the cross section of the multiple scattering at low angles (10°) to be ~ 60 mb sr^{-1} f.u.$^{-1}$ and ~ 40 mb sr^{-1} f.u.$^{-1}$ for the polycrystal and the single-crystal samples, respectively. In other measurements performed with 67 meV incident energy neutrons we also observed similar but slightly lower levels of multiple scattering, while at the lower incident energy of 17 meV the multiple scattering is rather weak. In the constant-Q scan at (0, 1.1, 1.1) of the triple-axis experiment[1] the incident energy varies from ~ 30 to ~ 60 meV for energy transfers covering the phononic energy range (0 to ~ 30 meV), going up to 110 meV at $\omega = 80$ meV. These energies being significantly higher than 17 meV would allow many phonon branches to be cut along $\sim 90°$ scattering angle and we should therefore expect a nonnegligible multiple-scattering contribution compared with the low-energy inelastic cross section which is only ~ 35 mb sr^{-1} f.u.$^{-1}$ over the measured energy range (0–80 meV).[1]

THE MAGNETIC CROSS SECTION

The cross section for an isotropic paramagnetic sample may be expressed as[22]

$$d^2\sigma/d\omega\ d\Omega = N(\gamma e^2/mc^2)^2[k'/k_0]S(Q,\omega), \qquad (2)$$

where N is the number of spins, $(\gamma e^2/mc^2)^2$ is the coupling constant (of magnitude 292 mb) between the neutron spin and the magnetic moment, k_0 and k' are the incoming and outgoing neutron wave vectors, and $S(Q,\omega)$ is the scattering function which describes the spin dynamics of the system. It is related to the imaginary part of the dynamic susceptibility $\chi''(Q,\omega)$ via the relation

$$S(Q,\omega) = (2\pi)^{-1}[1 - \exp(-\omega/T)]^{-1}\chi''(Q,\omega). \qquad (3)$$

The magnetic character of the high-energy spectral response of $CePd_3$ can be checked against the bulk susceptibility evaluated via the Kramers-Kronig integral of $S(Q,\omega)$, viz.,

$$\pi^{-1}\int \chi''(Q,\omega)\omega^{-1}d\omega = \chi(Q)F^2(Q) = 2\mu_B^2\int [1 - \exp(-\omega/T)] \times S(Q,\omega)\omega^{-1}d\omega, \qquad (4)$$

where $\chi''(Q,\omega)$ is the imaginary part of the dynamic susceptibility and $\chi(Q)$ is the static susceptibility with $[1-\exp(-\omega/T)]^{-1}$ representing the detailed balance factor and μ_B is the Bohr magneton. As mentioned earlier, a number of theories based on the large-N expansion[6,12,13] show that the ground state of the Anderson lattice can be represented to a very good approximation by a lattice of uncorrelated Kondo singlets. Hence we assume that the Q dependence results only from the *single-ion* magnetic form factor $F(Q)$ throughout.

In addition to the Kramers-Kronig integral the magnetic spectral response should also simultaneously satisfy the moment sum rule

$$\int S(Q,\omega)d\omega = A\mu_{\text{eff}}^2 F^2(Q), \qquad (5)$$

where the constant $A = 48.6$ mb sr^{-1} $\mu_B{}^{-2}$. Thus, if the $4f$ occupancy of the Ce^{3+} ion was integral we have $\mu_{\text{eff}} = \mu_0 = 2.54\mu_B$ and we expect $(Q \to 0)$ cross section of 314 mb sr^{-1} Ce^{-1}. In general, partial $4f$ occupancy $\langle n_f \rangle$ will be reflected in a lower cross section which implies a lower magnetic moment. We express this as

$$\mu_{\text{eff}}^2 = \mu_0^2\langle n_f \rangle. \qquad (6)$$

In the present experiment we have not been able to achieve a direct conversion of the data to the absolute scale using the vanadium sample due mainly to the fact that the latter was slab shaped (consisting of two plates of thickness 1 mm each) and larger compared with the $CePd_3$ samples which were cylindrical and hence illuminated differently by the nonuniform incident neutron beam. In other words, we are not able to estimate reliably the exact amount of vanadium exposed in the neutron beam, a prerequisite for evaluating absolute cross sections. We have therefore proceeded to convert the data to absolute scale indirectly via the susceptibility, by equating the Kramers-Kronig integral, Eq. (4), to the low-temperature bulk susceptibility measured earlier on the same polycrystalline sample.[3] The latter is, in fact, in excellent agreement with the Curie-Weiss-tail corrected low-temperature bulk susceptibility given by Kappler *et al.*[17] Using the intensity calibration so achieved we have evaluated the spectral integral and find it to be ~ 270 mb sr^{-1} Ce^{-1}, in good agreement with the absolute cross section of 280 ± 10 mb sr^{-1} Ce^{-1} determined directly relative to a vanadium standard in an independent experiment mentioned earlier.[21] The agreement between the two evaluations of the cross section is not surprising since the ratio of the susceptibility integral relative to the moment integral depends directly on the spectral shape and extent which is closely similar in the two cases. It is thus also evident why the spectral integral of the low-energy magnetic scattering observed by SSA,[1] which yields roughly the same static susceptibility as the high-energy response, should yield a moment which is only a small fraction (only $\sim$1/6th) of that obtained by integrating the latter response.

LOW-TEMPERATURE COHERENCE

Low-temperature physical properties of $CePd_3$ as for example, the Curie-Weiss upturn in the susceptibility below

$\sim$40 K,[17,19] which apparently correlates with the temperature below which the induced magnetic form factor shows a remarkable increase[23] are considered to mark the onset of coherence, and formation of quasiparticle bands at low temperatures. Similar observations of anomalies in the magnetic susceptibility and the form factor have been made in other valence fluctuation systems, for example, $CeSn_3$.[24,25] Additional evidence for the low-temperature coherent state was claimed by Lawrence, Thompson, and Chen,[18] from the electrical resistivity data of $CePd_3$ where an analysis of its temperature dependence following the relation $\rho=\rho_0+\rho'(T/T^*)^2$ yields a characteristic temperature T^* of similar magnitude ($\sim$45 K). The authors found also that below $\sim$40 K the resistivity was unaffected by an applied external pressure. Since the coherence is expected[26] to set in below a temperature $T_{\rm coh}\sim T_K/N$, where $N=2J+1=6$, consistency with this relation was claimed[18] by assuming that the Kondo temperature (or spin-fluctuation temperature) was given by $T_{\rm sf}\sim 2T_{\rm max}$, where $T_{\rm max}$ is the temperature of the maximum in the electrical resistivity. It was also suggested later,[27,28] that a similar magnitude of $T_{\rm sf}$ is indicated by the high-temperature ($T>200$ K) quasielastic Lorentzian half-width ($\sim$20 meV).[29,30] Strictly, however, the characteristic energy (at low temperatures) is represented by the centroid of the low-temperature inelastic Lorentzian i.e., $\sim$55 meV ($\sim$600 K) for $CePd_3$ observed directly from polarized neutron measurements.[2] A similar value $\omega_0\sim 50$ meV is obtained from the KMH fit which normally yields a slight underestimate of T_K.[6]

Others, for example, Mihalisin and co-workers[31,32] have argued that the onset of coherence is, in fact, represented by the down turn in the electrical resistivity. Thus for $CePd_3$ $T_{\rm max}$ ($\sim$120 K) the temperature of the maximum in the electrical resistivity may be taken as the coherence temperature. Adoption of this definition of coherence would appear consistent with the relation $T_{\rm coh}\sim T_K/N$ with $T_K\sim 600$ K suggested by the low-temperature neutron data of Galera *et al.*[2,3] which have been verified repeatedly in subsequent measurements[4,21] as well as in the present investigation. In later papers Lawrence, Chen, and Thompson,[27,28] have suggested that the low-temperature magnetic and resistivity phenomena (or anomalies) may be indicative of a *third* characteristic temperature scale for the system. This notwithstanding, we recall that the low-temperature Curie-Weiss upturn in the susceptibility itself has been interpreted differently by different workers. Kappler *et al.*[17] have claimed it to be an extrinsic effect found also in the diluted compounds $Ce_{1-x}Y_xPd_3$. The authors showed that the magnitudes of $\chi(0)$, after correction of the Curie-Weiss tail, followed a monotonic (almost linear) variation with x (for $x<0.4$). However others, for example Aarts *et al.*,[19] have argued that the Curie-Weiss upturn is an intrinsic property of the compound.

As for the present neutron data, it is evident that the observed single-ion spectral response of $CePd_3$ whose integrated intensity corresponds closely with the expected moment for the almost fully occupied Ce^{3+} state ($\langle n_f\rangle\sim 0.9$) and whose Kramers-Kronig integral accounts well for the bulk susceptibility (after correction for the Curie-Weiss tail) cannot be reconciled with the low-temperature coherence phenomena. This suggests that there may be additional features and/or contributions to the spectral response, besides the broad single-ion response observed clearly. In this connection we note the low-temperature Curie-Weiss upturn or tail often represents a significant fraction of the total susceptibility. Hence clearly, $\chi_{\rm tail}\sim\int[S(\omega)/\omega]d\omega$ is fairly large. However, if the tail was associated with low-energy processes such as those due to spin fluctuations from stable or nearly stable (i.e., low T_K) magnetic moments, the Kramers-Kronig integral can be quite large due to the factor $1/\omega$, while the spectral weight $\int S(\omega)d\omega$ associated with the tail can be fairly small relative to the broad high-energy response. The results obtained with 115 meV neutrons do not permit us to rule out the possibility of weak low-energy magnetic scattering particularly below $\sim$10 meV, the region ''shadowed'' by the large, resolution broadened elastic peak.

We have therefore investigated the low-energy region using neutrons of incident energy 17 meV, Fig. 5. In the Appendix we also show the Q-ω trajectories spanned with this incident energy for scattering angles of 10 and 90°. As discussed earlier, very few phonon branches are cut below $\sim$10 meV so that single-phonon or multiple-scattering processes should contribute extremely weakly to the low-energy region below $\sim$10 meV. The data for the single-crystal sample presented earlier in Fig. 5 show a very low level of additional scattering (black points) above that measured with the sample removed from its holder (diamonds). The difference signal represented by the open circles shows rather small additional scattering due to the sample itself within the energy range $2<\omega<10$ meV. The solid curve through the 17 meV data shows the magnetic scattering evaluated using the parameters of the fit to the ''phonon corrected'' high incident energy ($E_i=115$ meV) data. The magnetic intensity up to 10 meV represented by the fitted curve is only $\sim$1 mb sr^{-1} f.u.$^{-1}$, while the point by point integration of the signal over the energy range $2<\omega<10$ meV gives $\sim$2.5 mb sr^{-1} f.u.$^{-1}$. Again the lower limit (of $\sim$2 meV) for the latter integration is due to the region $-2<\omega<2$ meV being shadowed by the resolution broadened elastic peak.

The 17 meV data thus allow us to put an upper limit to the low-energy magnetic inelastic scattering within the energy range $2<\omega<10$ meV of $\sim$2.5 mb sr^{-1} f.u.$^{-1}$, which represents $\sim$1% of the cross section of the broad high-energy spectral response. Despite its low intensity, we mention as an illustration that if we evaluate the static susceptibility contribution due to this error signal assuming it to be approximated by a quasielastic distribution of width $\sim$3 meV, we find $\chi(0)\sim 0.2\times 10^{-3}$ emu mol^{-1} which is a non-negligible fraction of the Curie-Weiss upturn in the susceptibility at 10 K. Hence, low-energy processes originating from small amounts (consistent with the low spectral weight) of ''impurities'' or defect-stabilized (i.e., low T_K) Ce moments with spectral energies of the order of or smaller than $\sim$3 meV could quite plausibly account for the low-temperature susceptibility upturn. It is not excluded that a fraction of the Curie-Weiss tail or the susceptibility upturn may be due to intrinsic coherence effects which might influence the paramagnetic spectral response at much lower q's then so far accessed. In absence of theoretical guidance the problem appears complex, and is also complicated by the fact that the Curie-Weiss tail itself is strongly sample dependent, a fact

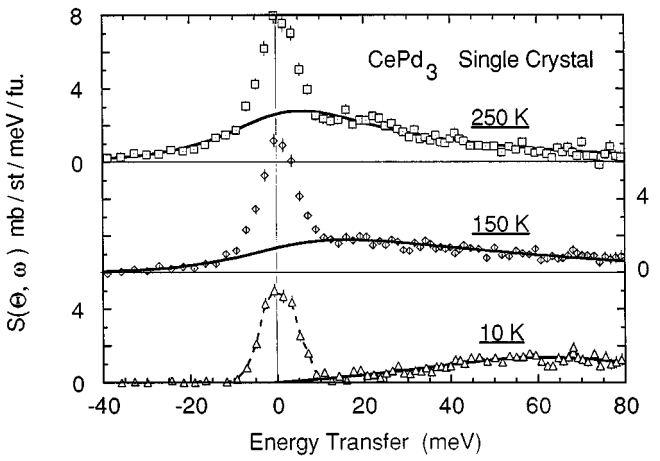

FIG. 9. Temperature evolution of the magnetic scattering from $CePd_3$ single crystal. The solid lines represent spectral fits to the data to a Lorentzian spectral distribution. At 10 K the Lorentzian is centered on ~53 (±5) meV with a spectral half-width of ~38 (±4) meV. At 150 K the spectrum is centered on zero energy (hence it is referred to as quasielastic distribution) of Lorentzian half-width 29 (±4) meV. The quasielastic Lorentzian half-width narrows to ~22 (±3) meV at 250 K.

often pointed out by a number of workers, e.g., Stassis *et al.*[23]

TEMPERATURE EVOLUTION

We have also investigated the temperature evolution of the paramagnetic spectrum of the single-crystal sample of $CePd_3$. In Fig. 9 we present the spectra at 10, 150, and 250 K measured with neutrons of incident energy 115 meV. The data have been corrected for the nonmagnetic contribution assuming it to be given by a fraction of the high angle ($\langle 2\Theta \rangle = 88°$) scattering where the optimum value of the fraction is slightly temperature dependent due to the evolution with increasing temperature of phonon scattering and hence also multiphonon and multiple-scattering contributions. The continuous curves through the data points represent the best fit assuming a single Lorentzian spectral component. As shown above at low temperatures the Lorentzian is centered on the characteristic Kondo energy of ~53 (±5) meV (while the KMH fit yields a value of $T_K \sim 50$ meV). At 150 K, i.e., around or just above the temperature of the maximum in the bulk susceptibility the magnetic spectral response is best represented by a Lorentzian centered on zero energy multiplied by the detailed balance factor [i.e., $\omega_0 = 0$ in Eq. 1(b)]. Such a response is generally referred to as quasielastic scattering although its spectral half-width is quite large, ~29 (±4) meV. We note that its apparent asymmetry around zero energy is due to the detailed balance factor, $[1-\exp(-\omega/T)]^{-1}$. At temperatures well above the maximum in the bulk susceptibility, i.e., at 250 K the quasielastic Lorentzian half-width decreases to ~22 (±3) meV, in good accord with $\Gamma \sim 20$ meV observed from the early neutron inelastic-scattering measurements on this compound using neutron energy gain spectroscopy (with cold neutrons) at moderately high temperatures ($T > 200$ K).[29,30]

CONCLUSIONS

The present measurements have clearly established the dominant role of strong multiple scattering at low Q values from the large samples of $CePd_3$, both polycrystalline as well as single crystal, used for measurements with moderate to high-energy thermal neutrons. We have demonstrated that the magnetic spectral response of the classic valence fluctuation compound $CePd_3$ is largely single-ion-like with a characteristic energy of ~50–55 meV (~600 K), thus reintegrating the compound to the family of valence-fluctuation systems showing a broad Lorentzian-like spectral response centered on characteristic energies ranging from ~100 K[7] to (at least) 2000 K.[11] This is consistent with a number of theories which show that for large degeneracies N the Kondo-lattice ground state is well approximated by a lattice of uncorrelated Kondo singlets. The present results which are in good agreement with earlier findings of Galera and co-workers[2,3] show also that *magnetic* scattering at low energies is relatively weak. Within the limits of our current knowledge it does not appear to us justified to interpret the low-temperature Curie-Weiss upturn (or a part of it) as indicating the onset of the low-temperature coherence. While one cannot rule out magnetic scattering due to intrinsic low-temperature coherence which may possibly occur at much lower q values than so far accessed, we have demonstrated how very weak scattering (of the order of or less than 2 to 3 % of the main response) due to magnetic impurities or, most likely, defect-stabilized Ce moments with T_K's less than 2 or 3 meV (i.e., 20 or 30 K) could quite adequately account for the low-temperature Curie-Weiss tail in the susceptibility.

ACKNOWLEDGMENTS

The authors acknowledge B. Dorner for many informative discussions as well as comments on the manuscript and also thank J. Kulda, N. Pyka, and H. Schober for helpful discussions. We acknowledge the loan of the single-crystal sample from S. M. Shapiro and C. Stassis and thank them as well as G. Aeppli, R. M. Galera, and J. Pierre for discussions and their interest in this work.

APPENDIX

In Fig. 10 we show the scattering diagram in the reciprocal space for the constant-q scans of SSA (Ref. 1) and in Fig. 11 for the present tof experiment in which the incident wave vector $\mathbf{k_i}$ was along the [0,1,1] direction. Changing the sample orientation through 15° resulted in no noticeable change in the scattering at low angles (10°). Also, the changes were relatively small for the group of detectors around the reference angle of 90°, although at intermediate angles the changes were more pronounced as phonon-dispersion curves were ''cut'' or avoided due to the changes

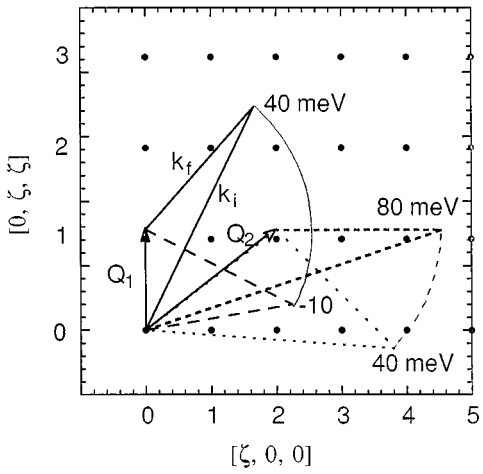

FIG. 10. The scattering diagrams for the three-axis measurements showing the scattering plane bound by the $[0,\zeta,\zeta]$ and $[\zeta,0,0]$ axes. The scattering vectors $\mathbf{Q_1}$ and $\mathbf{Q_2}$ remain constant and the arcs represent the locii of the wave vectors $\mathbf{k_i}$ and $\mathbf{k_f}$ along the scan, with the magnitude of k_f ($=3.83$ Å^{-1}) remaining constant throughout.

in the directions of $\mathbf{k_i}$ and $\mathbf{k_f}$. Since the scattering vector Q is relatively small at low angles, the single-phonon intensity (proportional to Q^2) is small in comparison with the multiple-scattering processes which are dominant and practically invariant with sample orientation at these low angles.

In Fig. 12 the dotted curves show the Q-ω trajectories followed in the present tof experiment with neutrons of incident energy 115 and 17 meV. In the figure we have also included the phonon-dispersion curves along the $[0,\ \zeta,\ \zeta]$ direction for $CePd_3$.[5] The thick solid line at $Q=(0,\ 1.1,\ 1.1)$ represents the low-energy constant-q scan in the three-axis measurements of SSA.[1] For simplicity we show the higher-energy scan at $Q=(0,\ 2.1,\ 2.1)$ rather than at $Q=(2,\ 1.1,\ 1.1)$ actually performed by SSA.[1] Although $\mathbf{q}$ is the same, i.e., (0, 0.1, 0.1) for the two points in the reciprocal space the magnitudes $|Q|$ are slightly different. We note also that in the tof experiment the scattering vector $\mathbf{Q}$ does not lie along the $[0,\zeta,\zeta]$ direction but rather varies (in a compex manner) with the energy transfer ω. However, with respect to the phonon branches the illustration is qualitatively similar for the other two principal directions also. Figure 13 represents a part of Fig. 12 plotted on an expanded scale to highlight the Q-ω trajectories followed by the 17 meV neutrons. Evidently the

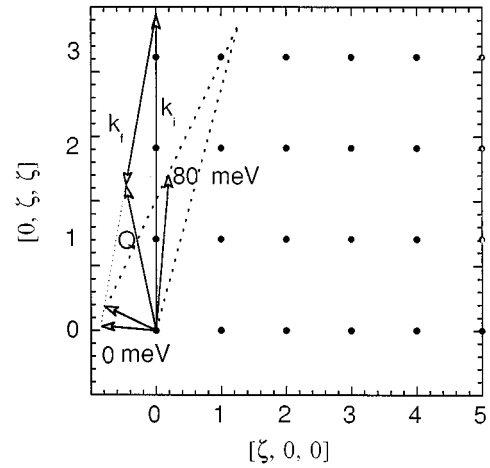

FIG. 11. The scattering diagrams corresponding to the low angle scan in the time-of-flight experiment with the incident wave vector $\mathbf{k_i}$ along $[0,\zeta,\zeta]$ and oriented 15° away. The wave vector $\mathbf{Q}$ varies in magnitude and direction within the scattering plane as a function of the energy transfer.

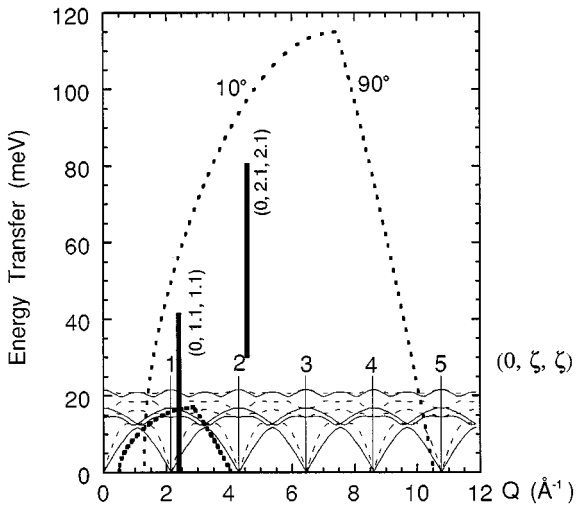

FIG. 12. The Q-ω trajectories for the time-of-flight experiment for the two reference scattering angles of 10° and 90° for neutrons of incident energy 115 meV (dotted lines) and 17 meV (thick dotted lines). The thin solid lines and dashed lines represent the phonon dispersion curves for $CePd_3$ along $[0,\zeta,\zeta]$ repeated over several Brillouin zones. The thick vertical line at (0, 1.1, 1.1) represents the low energy ($-10<\omega<40$ meV) constant-Q scan in the three-axis measurements of SSA (Ref. 1). For simplicity, we have also included a second thick line at (0, 2.1, 2.1) which is qualitatively equivalent to the scan actually performed by SSA (Ref. 1) at (2, 1.1, 1.1) over the energy range ($30<\omega<80$ meV).

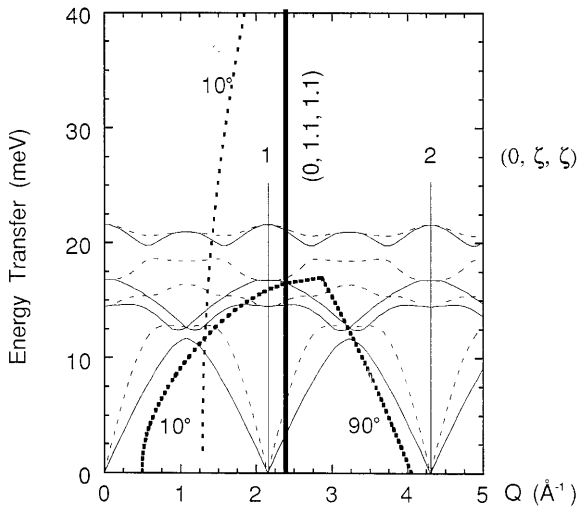

FIG. 13. A part of Fig. 12 plotted on expanded vertical and horizontal scales.

low angle detectors at 10° do not cut any phonon branches below ~10 meV along the $[0,\zeta,\zeta]$ direction. The situation is not too different along the other two principal directions. Similarly the Q-ω trajectory for the 90° scattering angle also avoids low-energy phonons thus greatly reducing low-energy multiple-scattering contributions at low angles since these arise dominantly via processes in which the first scattering events are along 90°, the long axis of the cylindrical samples.

[1] S. M. Shapiro, C. Stassis, and G. Aeppli, Phys. Rev. Lett. **62**, 94 (1989).

[2] R. M. Galera, D. Givord, J. Pierre, A. P. Murani, C. Vettier, and K. R. A. Ziebeck, J. Magn. Magn. Mater. **47&48**, 139 (1985).

[3] R. M. Galera, A. P. Murani, J. Pierre, and K. R. A. Ziebeck, J. Magn. Magn. Mater. **63&64**, 594 (1987).

[4] A. Severing and A. P. Murani, Physica B **163**, 699 (1990).

[5] A. Severing, W. Reichardt, E. Holland-Moritz, D. Wohlleben, and W. Assumus, Phys. Rev. B **38**, 1773 (1988).

[6] Y. Kuramoto and E. Müller-Hartmann, J. Magn. Magn. Mater. **52**, 122 (1985).

[7] A. Severing, A. P. Murani, J. D. Thompson, Z. Fisk, and C.-K. Loong, Phys. Rev. B **41**, 1739 (1990).

[8] A. P. Murani, J. Phys. C **33**, 6359 (1983).

[9] A. Severing, E. Gratz, B. D. Rainford, and K. Yoshimura, Physica B **163**, 409 (1990).

[10] C.-K. Loong, B. H. Grier, S. M. Shapiro, J. M. Lawrence, R. D. Parks, and S. K. Sinha, Phys. Rev. B **35**, 3092 (1987).

[11] A. P. Murani, Z. A. Bowden, A. D. Taylor, R. Osborn, and W. G. Marshall, Phys. Rev. B **48**, 13 981 (1993).

[12] T. V. Ramakrishnan and K. Sur, Phys. Rev. B **26**, 1798 (1982).

[13] P. Coleman, Phys. Rev. B **28**, 5255 (1983).

[14] M. Croft, R. Neifeld, C. U. Segre, S. Raaen, and R. D. Parks, Phys. Rev. B **30**, 4164 (1984).

[15] E. Beaurepaire, G. Krill, and J. P. Kappler, Solid State Commun. **49**, 65 (1984).

[16] R. D. Hutchens, V. U. S. Rao, J. E. Greedan, and R. S. Craig, J. Phys. Soc. Jpn. **32**, 451 (1972).

[17] J. P. Kappler, G. Krill, M. J. Besnus, M. F. Ravet, N. Hamdaoui, and A. Meyer, J. Appl. Phys. **53**, 2152 (1982).

[18] J. M. Lawrence, J. D. Thompson, and Y. Y. Chen, Phys. Rev. Lett. **54**, 2537 (1985).

[19] J. Aarts, F. R. de Boer, P. F. de Chatel, and A. Menovsky, Solid State Commun. **56**, 623 (1985).

[20] D. Malterre, M. Grioni, P. Weibel, B. Dardel, and Y. Baer, Phys. Rev. Lett. **68**, 2656 (1992).

[21] A. P. Murani, R. Raphel, Z. A. Bowden, and R. S. Eccleston (unpublished).

[22] W. Marshall and R. D. Lowde, Rep. Prog. Phys. **31**, 705 (1968).

[23] C. Stassis, C.-K. Loong, O. D. McMasters, R. M. Moon, and J. Thompson, J. Appl. Phys. **53**, 7890 (1982).

[24] C. Stassis, C.-K. Loong, B. N. Harmon, S. H. Liu, and R. M. Moon, J. Appl. Phys. **50**, 7567 (1979).

[25] J.-X. Boucherle, G. Fillion, J. Flouquet, F. Givord, P. Lejay, and J. Schweizer, J. Magn. Magn. Mater. **62**, 277 (1986).

[26] P. W. Anderson, in *Valence Fluctuations in Solids*, edited by L. M. Falicov, W. Hanke, and M. B. Maple (North-Holland, Santa Barbara, 1981), p. 451.

[27] J. M. Lawrence, Y. Y. Chen, and J. D. Thompson, Phy. Rev. Lett. **55**, 1702 (1985).

[28] J. Lawrence, Y. Y. Chen, and J. Thompson, in *Theoretical and Experimental Aspects of Valence Fluctuations and Heavy Fermions*, edited by L. C. Gupta and S. K. Malik (Plenum, New York, 1987), p. 169.

[29] M. Loewenhaupt and E. Holland-Moritz, J. Appl. Phys. **50**, 7456 (1979).

[30] E. Holland-Moritz, D. Wohlleben, and M. Loewenhaupt, Phys. Rev. B **25**, 7482 (1982).

[31] T. Mihalisin and J. E. Crow, Phys. Rev. Lett. **55**, 1701 (1985).

[32] P. Scoboria, J. E. Crow, and T. Mihalisin, J. Appl. Phys. **50**, 1895 (1979).